Supplementary information

Evaluation of fluorine and Sulfonic acid co-functionalized graphene oxide membranes under hydrogen proton exchange membrane fuel cell conditions

Robin Sandström[a], Alagappan Annamalai[a], Nicolas Boulanger[a], Joakim Ekspong[a], Alexandr Talyzin[a], Inge Mühlbacher[b], Thomas Wågberg[a,*]

[a]Department of Physics, Umeå University, Umeå 90187, Sweden

[b]Polymer Competence Center Leoben GmbH PCCL, Leoben 8700, Austria

Pre-oxidation of flake graphite powder

Natural flake graphite (Sigma Aldrich, +100 mesh, Lot# MKBS2224V) was first pre-oxidized by mixing 3 g graphite powder together with 2.5 g Potassium persulfate ($K_2S_2O_8$) and 2.5 g Phosphorous pentoxide (P_4O_{10}) were dispersed in 24 ml concentrated Sulfuric acid (97-98%, H_2SO_4). The mixture was maintained at 80 ^oC in an oil bath for 4 h under stirring, followed by washing through filtering with copious amounts of distilled water $(H_2O)_{DI}$ until a neutral pH was achieved. After completely drying the product in vacuum at 80 ^oC overnight, the pre-oxidized graphite was then used for synthesis of HGO, TGO* and F-TGO.

Synthesis of HGO

To synthesize HGO, 3 g the pre-oxidized graphite was dispersed in 120 ml H_2SO_4 with 1.5 g Sodium nitrate ($NaNO_3$) followed by a slow addition of 9 g of Potassium permanganate ($KMnO_4$) via a funnel over the course of approximately 30 min under vigorous stirring in an ice bath. The reaction mixture was kept in the ice bath for 2 h after which the temperature was raised to 35 ^oC and maintained for an additional 2 h. Now, 120 ml of $(H_2O)_{DI}$ was carefully added upon which a strong exotherm was observed. After maintaining the mixture at a temperature of 98 ^oC for 15 min, an additional 300 ml H_2O was added followed by 18 ml Hydrogen peroxide (H_2O_2). Thereafter the mixture was washed according to the same procedure as all other samples described in the manuscript.

Nafion (N211) pre-treatment

All Nafion 211 membranes (N211) were pretreated before use. The treatment consisted of subsequent heating of the as-received membranes at 80 ^{o}C for 1 h each in $(H_2O)_{DI}$, 3 % H_2O_2, $(H_2O)_{DI}$, 0.5 M H_2SO_4 and finally $(H_2O)_{DI}$. The membranes were then stored in $(H_2O)_{DI}$ until usage.

Supporting characterization details

Raman spectra were acquired by a Renishaw InVia Raman spectrometer with a laser excitation wavelength of 514 nm. Scanning electron microscopy imaging was performed with a Zeiss Merlin field emission SEM at 4 kV accelerating voltage and a current of 100 pA. Transmission electron microscopy was performed using a Jeol 1230 microscope (80 kV). Zeta potential measurements were performed with a Litesizer^{TM} 500 (Anton Paar) by first diluting 200 µl of the 0.5 mg ml^{-1} dispersions in 10 g of 1 mM KNO_3 solution where pH was adjusted with either 0.05 M KNO_3 or 0.05 M KOH. Data points considered obvious outliers (particularly those having high standard deviations) were removed followed by a polynomial fit to the second order for trend-comparison purposes. TGO* could not be measured due to too large standard deviation at all pH.

Ion-exchange capacity (IEC) measurements were performed on the F-TGO and SF-TGO samples by first equilibrating the membranes in 1 M NaCl solution for 48 h. Thereafter a solution of 0.01 M NaOH was slowly added until neutralized. The IEC (in mmol/g), was then calculated according to:

$$IEC = \frac{Consumed\ NaOH\ solution * NaOH\ concentration}{Membrane\ weight} \quad . \qquad \text{(S1)}$$

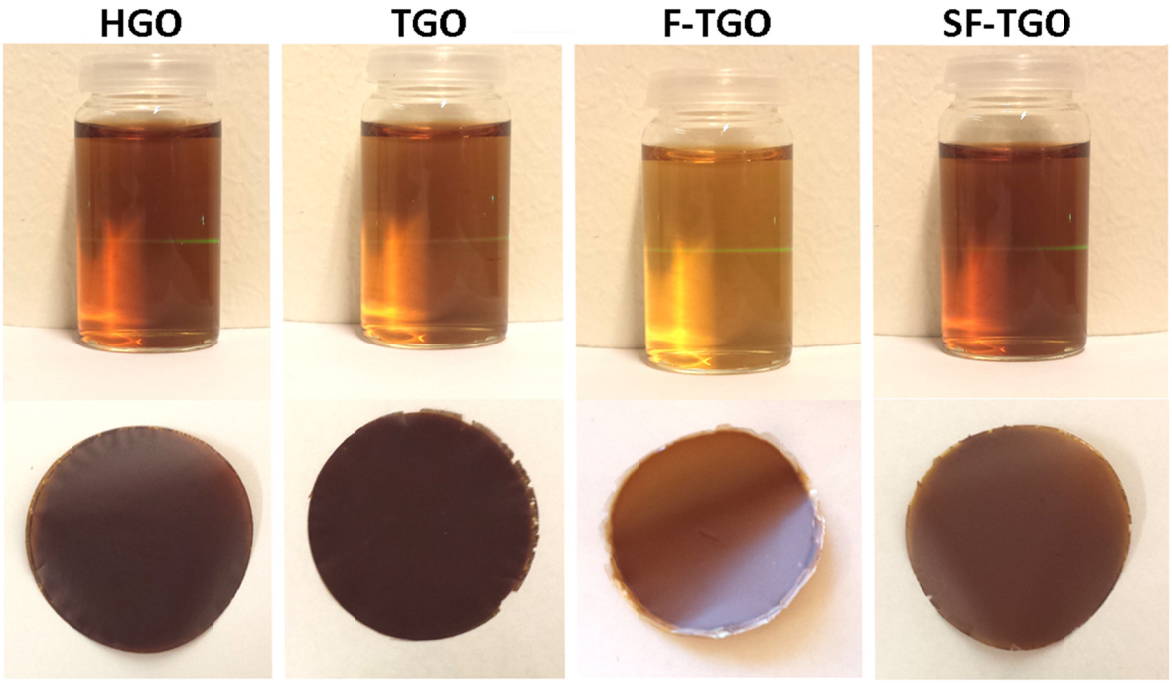

Fig. S1. *Images depicting respective dispersions (0.5 mg ml^{-1}) and resulting membranes. TGO and TGO* looked identical (visually).*

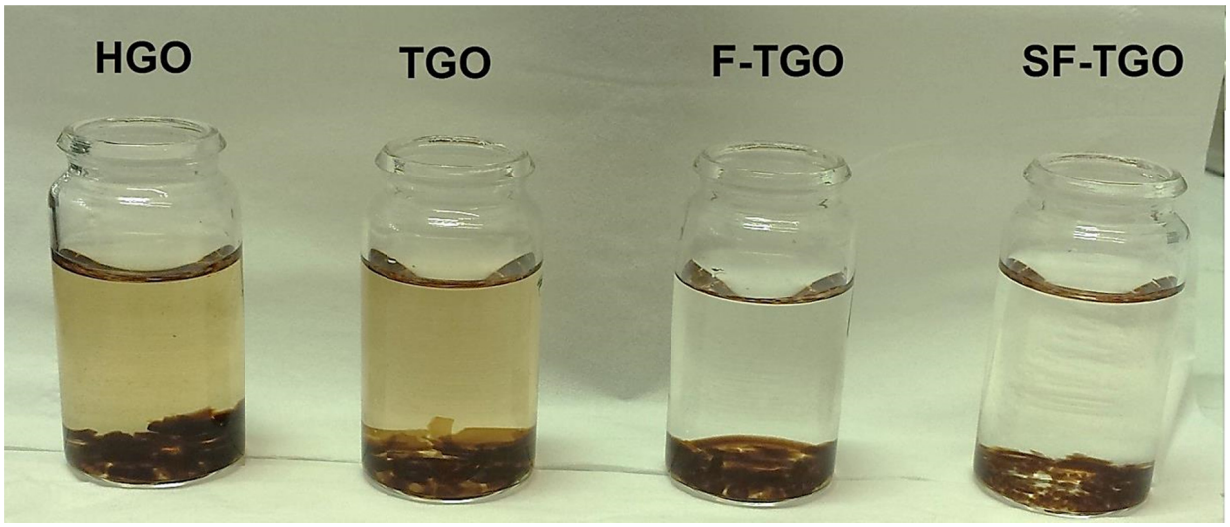

Fig. S2. *Pieces of membranes stored for three (3) days in neutral water. HGO and TGO slowly visibly dispersed while F-TGO and SF-TGO remained stable. TGO* had identical behavior as TGO.*

Table S1. *Average thicknesses as measured by a digital micrometer tool at various locations on the membrane. The variation for all membranes was about +/- 2 µm.*

HGO	*TGO*	*TGO**	*F-TGO*	*SF-TGO*
9 µm	*9 µm*	*7 µm*	*9 µm*	*8 µm*

Table S2. *2θ Positions of the C(002) reflections. The position when membranes are soaked in $(H_2O)_{DI}$ are shown in parenthesis.*

HGO	*TGO*	*TGO**	*F-TGO*	*SF-TGO*
10.9 (6.0)	*10.9 (6.1)*	*11.2 (5.5)*	*10.3 (6.0)*	*10.8 (6.1)*

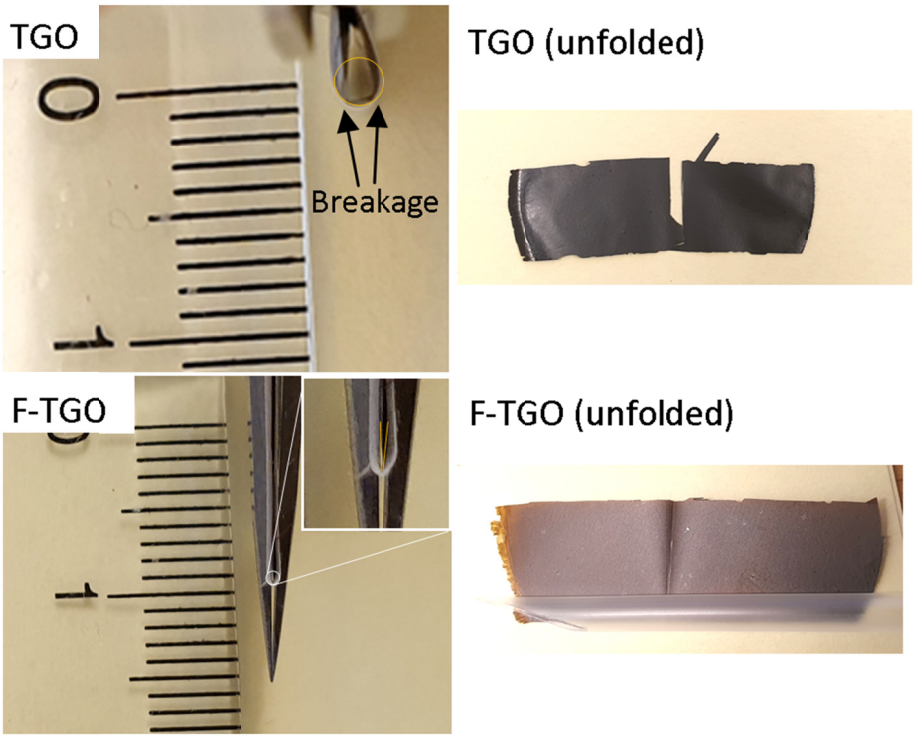

Fig. S3. *Estimation of the bend radius of dry 1 cm wide strips of TGO (top) and F-TGO (bottom) by first encapsulating them with thin paper (baking paper) while slowly reducing the radius with a tweezer until breakage could be observed. For TGO, breakage was first observed at a bend radius of ~0.9 mm whereas F-TGO could be completely folded with the tweezer without breakage as shown in the image of the unfolded strip. Thus, the flexibility and consequently the "handleability" was clearly improved as a result of fluorination.*

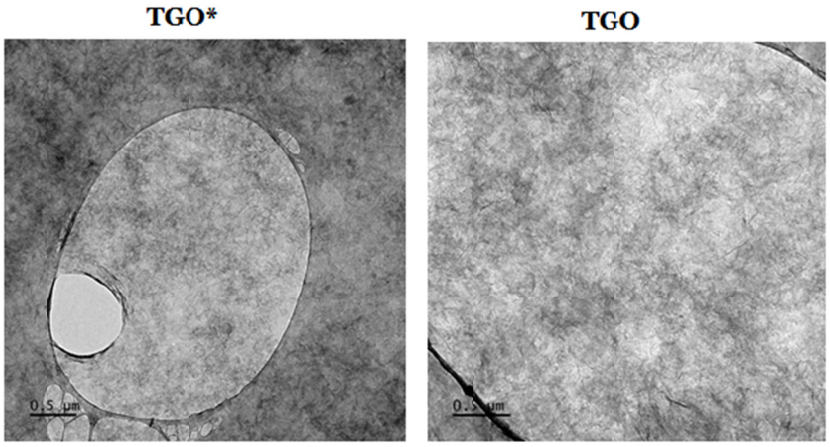

Fig. S4. *TEM images comparing a TGO* and TGO flake. TGO* typically showed regions with perforated flakes such as in the presented image, possibly indicating that TGO* was over oxidized.*

Table S3. *Summary of X-ray photoelectron spectroscopy data including atomic percentages given by the C 1s, F 1s and S 2p core-level regions.*

	Binding Energy [eV]	HGO [at. %]	TGO* [at. %]	TGO [at. %]	F-TGO [at. %]	SF-TGO [at. %]	Likely attributed species
C 1s	283,8	2,99	3,39	6,54	3,24	4,69	Unidentified
C 1s	285,0	21,76	16,35	15,54	15,90	16,84	C-CH, C=C
C 1s	287,0	37,64	35,44	37,11	40,34	39,67	C-OH, epoxides
C 1s	288,4	3,51	3,93	4,82	3,97	3,99	C=O
C 1s	289,1	2,56	4,05	2,04	3,51	1,28	carboxyl
F 1s	686,5	-	-	-	0,53	0,41	Semi-ionic F, HF
S 2p $_{3/2}$	168,2	0,17	0,22	0,16	0,13	0,55	SO_3^-
S 2p $_{3/2}$	169,5	0,15	0,09	0,28	0,09	-	Protonated (SO_3H or H_2SO_4)
C/O ratio	-	2.2	1.7	2.0	2.1	2.1	-

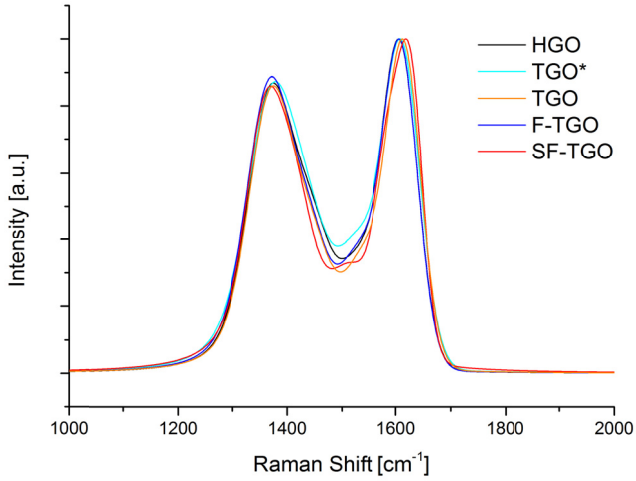

Fig. S5. *Raman spectra (fitted with a four-peak model) showing near-identical D/G ratio (~0.9) for all samples. The methods sensitivity was not adequate to see an increased disorder in TGO* despite the lower C/O ratio as measured by XPS.*

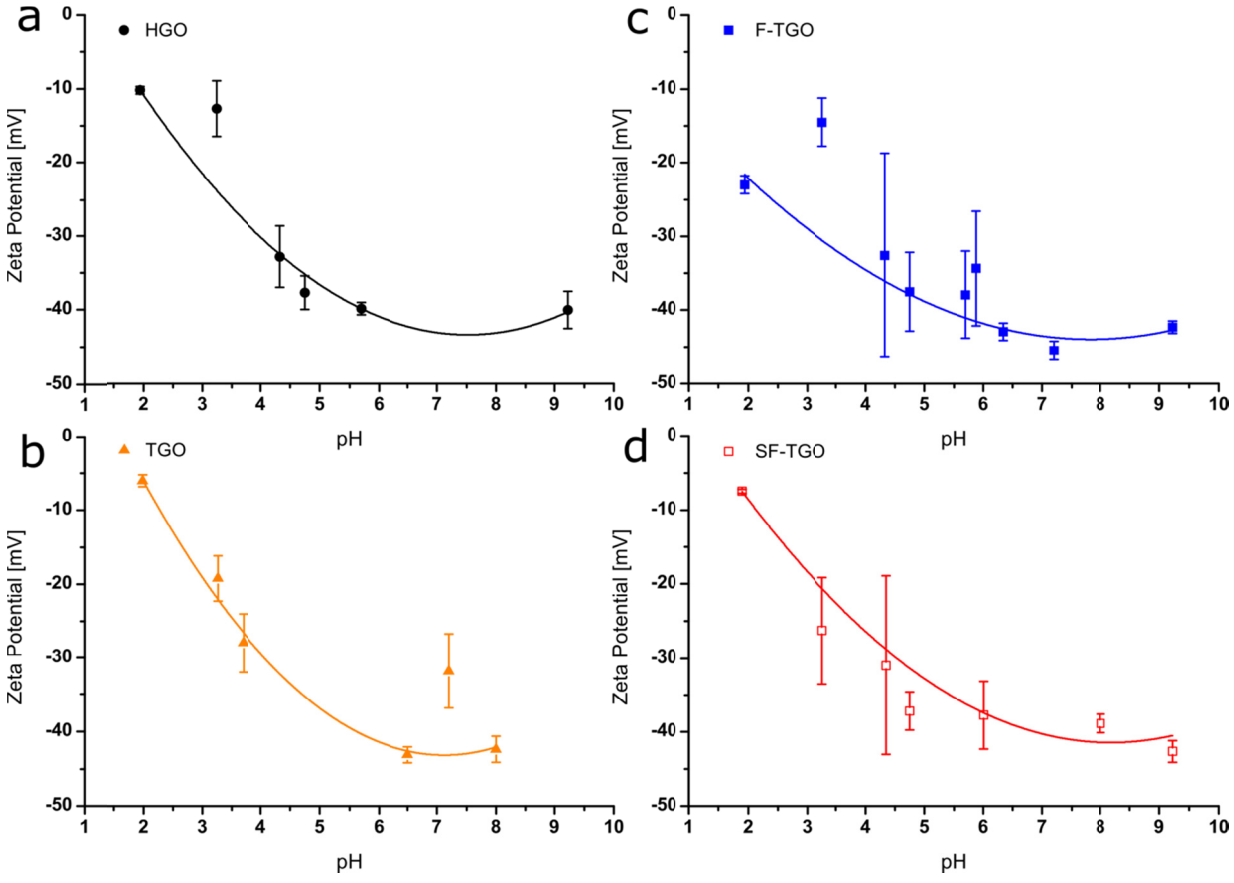

Fig. S6. *Zeta potential measurements of respective dispersion. Outliers are removed and the trend shown are of a second order polynomial best-fit. TGO* could not be measured.*

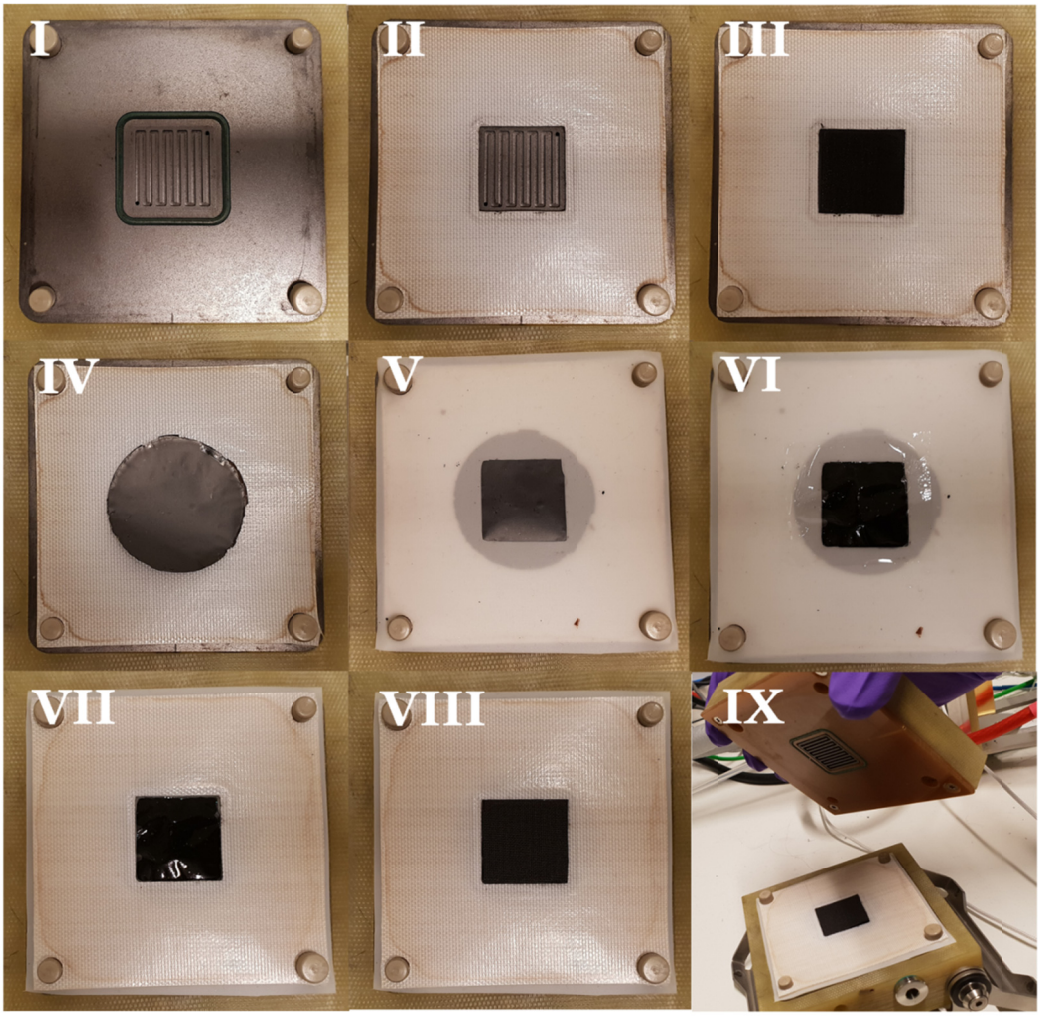

Fig. S7. *MEA fabrication steps prior to recording the polarization curves in Fig. 6. First, the anode GDE was placed on the anodic flow field (current collector) and fixated with a teflonized fiberglass gasket (I-III). Second, The GO membrane was fixated with a thin silicon rubber gasket (IV-V). The N211 membrane could then be easily placed and fixated with an additional teflonized fiberglass gasket (VI-VII) and finally assembled together with the cathode GDE + flow fields (VIII-IX).*

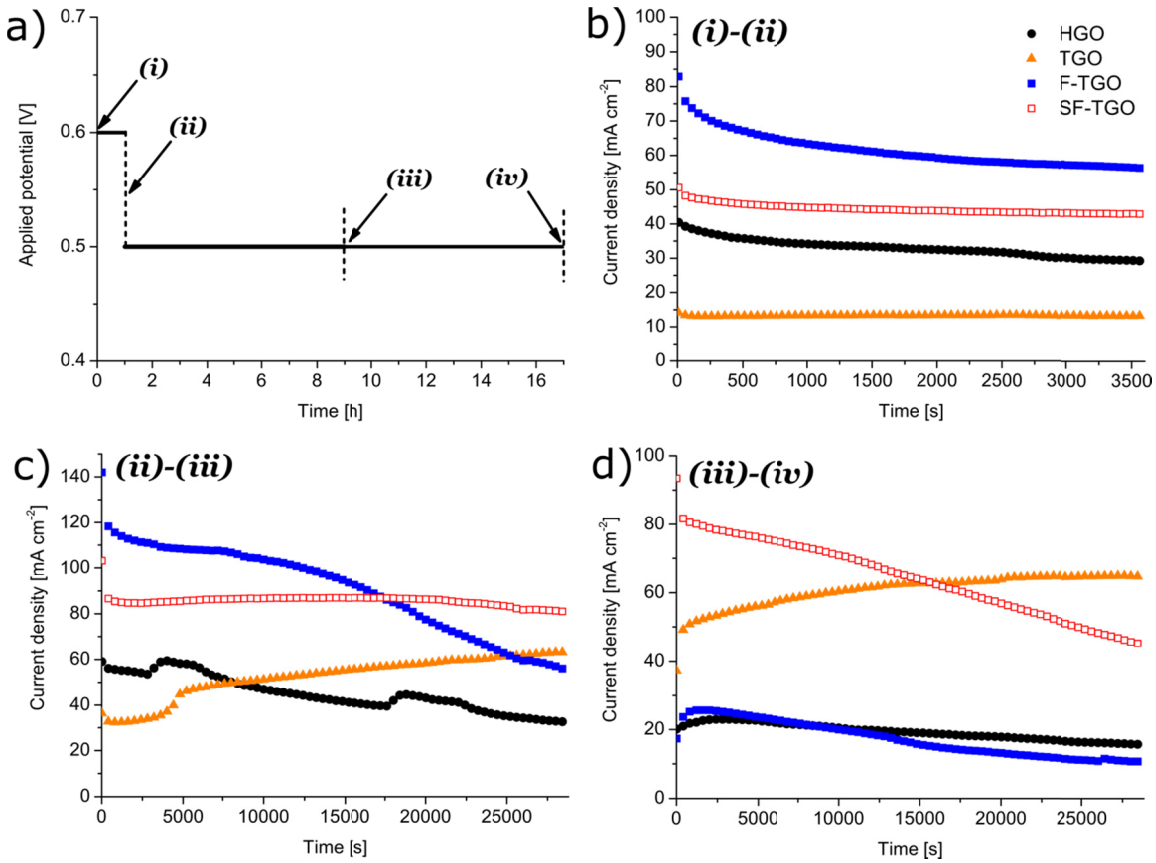

Fig. S8. *Current vs. time curves (constant potential) corresponding to the four events (a) on which the polarization curves in Fig. 6 was recorded.*

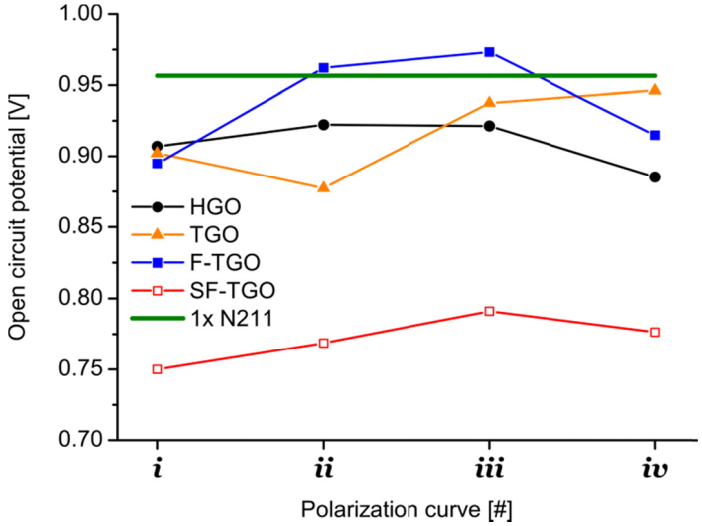

Fig. S9. *Temporal evolution of the open circuit potential prior to respective deactivation shown in Fig. 6 and Fig. S8. Stable OCP of a single N211 membrane was measured to 0.957 V (green line).*

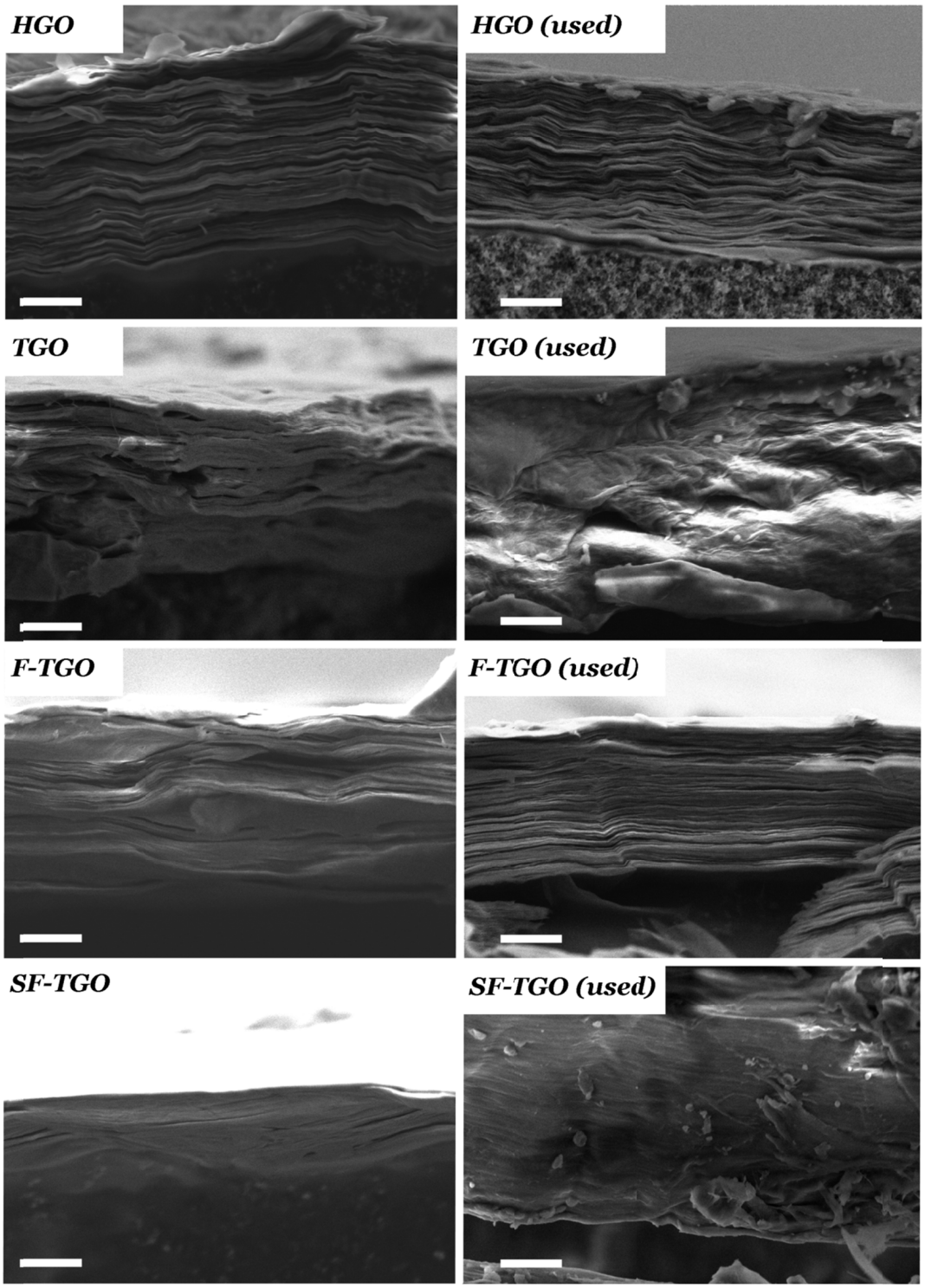

Fig. S10. *SEM images of as-synthesized and used membranes after fuel cell operation (Scale bar: 2 µm). Images were acquired with an in chamber secondary electron detector. Charging effects in particularly SF-TGO caused imaging at higher resolution to be problematic, but rendered images clear enough for detection of severe disruptions to the laminar framework.*

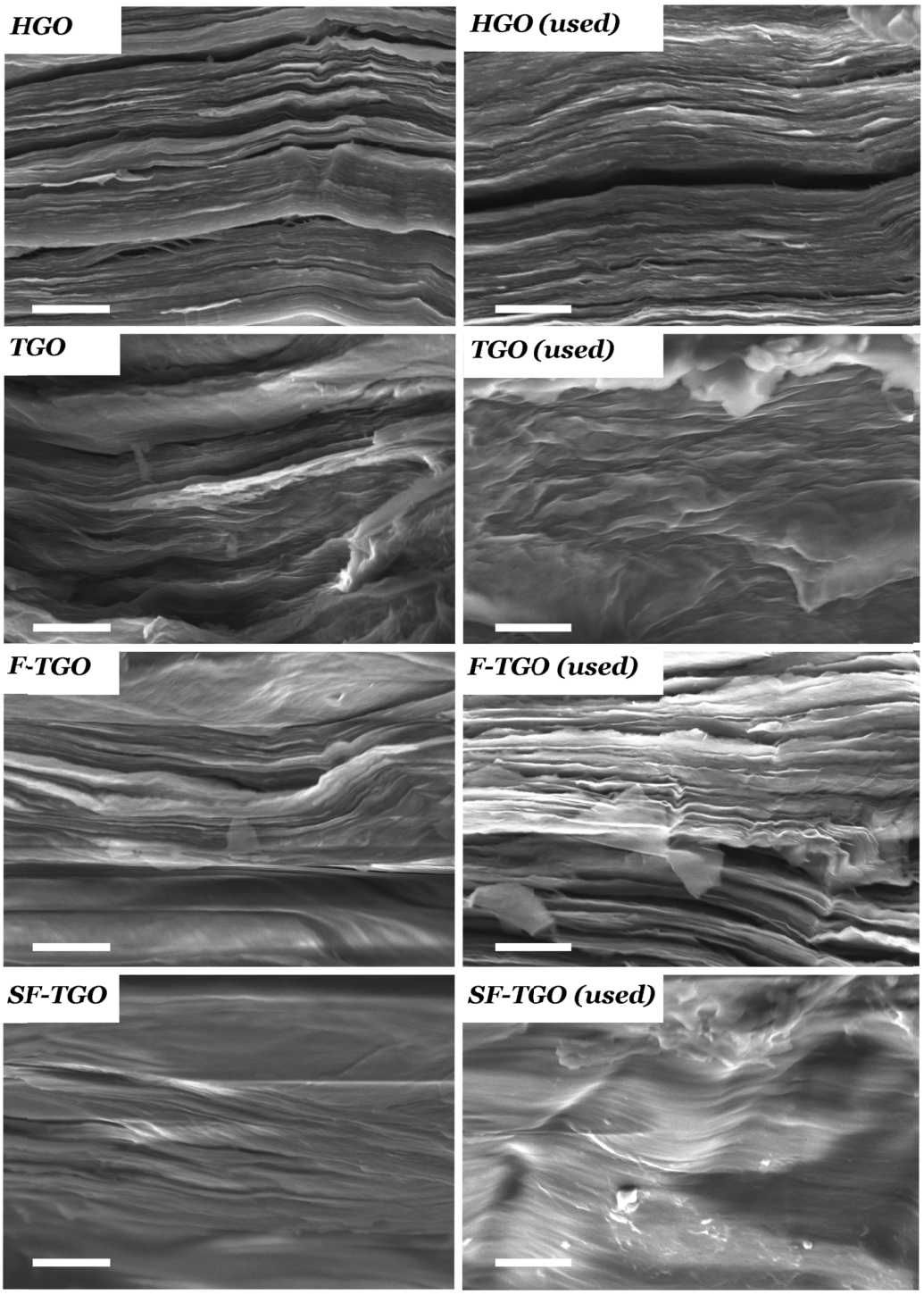

Fig. S11. *SEM images of as-synthesized and used membranes after fuel cell operation (Scale bar: 1 µm). Images were acquired with an in lens secondary electron detector. Charging effects in particularly SF-TGO caused imaging at higher resolution to be problematic, but rendered images clear enough for detection of severe disruptions to the laminar framework.*